

Experimental Observation of Laser-Induced Radiation Heat Waves

R. Sigel, G. D. Tsakiris, F. Lavarenne, J. Massen, R. Fedosejevs,^(a) J. Meyer-ter-Vehn, M. Murakami,^(b)
K. Eidmann, and S. Witkowski

Max-Planck-Institut für Quantenoptik, D-8046 Garching, Federal Republic of Germany

H. Nishimura, Y. Kato, H. Takabe, T. Endo, K. Kondo, H. Shiraga, S. Sakabe, T. Jitsuno, M. Takagi,
C. Yamanaka, and S. Nakai

Institute of Laser Engineering, Osaka University, Suita, Osaka 565, Japan

(Received 30 April 1990)

The propagation of a radiation heat wave through a thin foil of solid gold was investigated experimentally. The wave is driven by the intense thermal radiation in 1–3-mm-diam gold cavities heated by an intense laser pulse (duration 0.8–0.9 ns, wavelength 0.35 μm) to temperatures of more than 200 eV. Evidence of the propagating wave was obtained from the delayed onset of intense thermal emission from the outer side of the foil. The results agree with theoretical predictions for a self-similar ablative heat wave and with numerical simulations.

PACS numbers: 52.50.Jm, 44.40.+a, 47.70.Mc

Marshak¹ was apparently the first to notice that under conditions of complete local thermodynamic equilibrium between radiation and matter the diffusion of intense thermal radiation into an optically thick wall leads to the formation of a radiation heat wave. Such waves play an important role in high-temperature hydrodynamic phenomena.² Their investigation in the laboratory became possible with the advent of modern pulsed power sources, in particular lasers, allowing the generation of intense, isotropic thermal radiation with brightness temperatures in excess of 10^6 K.^{3–8}

In this Letter we report for the first time the observation of radiation heat waves driven by intense laser-generated soft x rays. As shown schematically in Fig. 1(a), the x rays impinge on the front side of a thin gold foil and drive a heat wave through it. Because of the strong increase of radiation heat conductivity with temperature the heat wave has a sharp front followed by a temperature plateau. Evidence of the propagating wave is obtained by observing the sudden onset of intense x-ray emission from the rear side of the foil [Fig. 1(b)].

As driving radiation we use the isotropic and approxi-

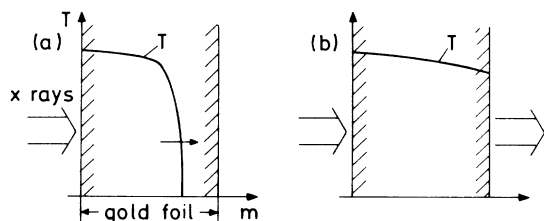


FIG. 1. (a) Propagation of an x-ray-driven radiation heat wave through a thin gold foil; m is the mass coordinate. (b) After arrival of the wave the rear side of the foil emits intense thermal radiation.

mately Planckian radiation generated in a laser-heated gold cavity (see Fig. 2). Besides holes for the laser beams such a cavity has a pair of diagnostic holes. One carries the sample foil, while the other serves as an open reference hole which allows simultaneous measurement of the radiation in the cavity. It should be noted that the closed geometry of a cavity provides uniform and, at the same time, intense irradiation under conditions close to complete thermodynamic equilibrium, which is not easily achieved by other configurations. In open geometry, only qualitative evidence of the formation of a radiation heat wave has been obtained so far, at a much lower flux level.^{9,10}

In our experiment the foil and cavity are both made of gold and the foil forms part of the cavity wall. The radiation heat wave penetrating both of them is of the ablative type and can be described by a self-similar solution.¹¹ For a completely closed cavity the scaling laws for the penetration depth d_f into solid gold (density 19.3

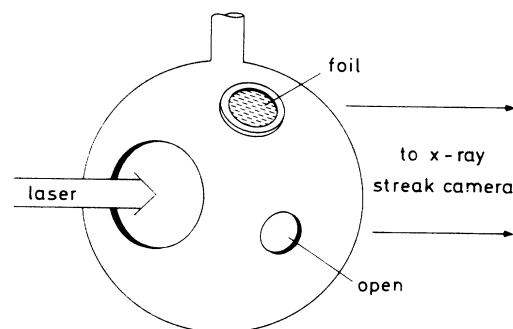


FIG. 2. Schematic representation of a laser-heated cavity with a thin gold foil mounted on one hole and with an open reference hole.

g cm^{-3}) and the temperature are¹²

$$d_f = 3.3 S_s^{7/13} t^{10/13} \mu\text{m}, \quad (1)$$

$$T = 267 S_s^{4/13} t^{2/13} \text{eV}. \quad (2)$$

Here the temporally constant source flux S_s is in units of 10^{14}W cm^{-2} , time t in units of 10^{-9}s , and S_s is given by the fraction of the laser power converted into x rays, divided by the inner surface of the cavity. The Rosseland opacity for gold calculated in the average-ion approximation was used in evaluating the scaling laws.¹³ Holes in the cavity wall cause additional losses and weaken the radiation field in the cavity. In the presence of holes S_s in Eqs. (1) and (2) should be multiplied by a correction factor $1 - n^{-1} S_r(t)/S_s$, where n^{-1} is the fractional hole area and $S_r = \sigma T^4$ the flux reemitted from the hot cavity wall. $S_r(t)$ may be calculated as described in Ref. 8. The effect of holes is noticeable only in the smallest cavities used in the present experiments.

Experiments were carried out with up to ten beams (in two bundles of five) of frequency-tripled $\lambda = 0.35 \mu\text{m}$ radiation from the Gekko XII Nd-glass laser facility. The maximum pulse energy was 5 kJ and the pulse duration 0.8–0.9 ns. The majority of experiments were carried out with spherical gold cavities 3, 2, or 1 mm in diameter. The diameters of the diagnostic holes were 250 μm (3 mm cavity), 150 μm (2 mm cavity), and 100 μm (1 mm cavity). The thin gold foils were fabricated separately by electroplating. Reinforced on one side by an electroplated gold ring with an inner diameter slightly larger than the diagnostic hole diameter, they were fixed on their flat side with a thin layer of glue (less than 2 μm thick) on the outer side of the 10- μm -thick cavity wall. Prior to the detachment from the substrate, the mass per unit area of the gold foil was determined with 2% accuracy by weighing the substrate before and after electroplating.

The temporal evolution of the radiation from the hole covered by the gold foil and that from the open reference hole were measured simultaneously at a fixed wavelength. The two holes were projected through two crossed slits, located at different positions, with spatial and spectral resolution onto the cathode slit of an x-ray streak camera (XRSC). The position of the second slit, covered with a transmission diffraction grating, could be varied in order to choose the observed wavelength. The temporal resolution was $\lesssim 30 \text{ps}$ and the observed bandwidth about 6 \AA . Time-integrated, space-resolved spectra from both holes were obtained in the range 5–150 \AA with the help of pinhole transmission-grating spectrometers (PTGS) which used absolutely calibrated x-ray film¹⁴ as detector. On the opposite side of the cavity a time-resolving spectrograph, consisting of a transmission grating and an XRSC, recorded the cavity spectrum radiated through another open diagnostic hole. With the calibration provided by the spectra of an additional

PTGS, this instrument yielded the brightness temperature of the cavity as a function of time.

A total of fifteen experiments were performed with the average laser flux S_L (incident laser power divided by the inner surface of the cavity) covering the range 6×10^{12} to $2 \times 10^{14} \text{W cm}^{-2}$ and with foils from 0.25 to 1.37 μm thick.

Figure 3(a) shows isointensity contours of the signal on the screen of the XRSC for an experiment where a 0.91- μm -thick gold foil was mounted on a 1-mm-diam cavity. The observed wavelength was 60 \AA . Figure 3(b) shows the evolution of the x-ray intensity with time. It is clearly seen that the radiation from the foil begins with a delay. It is interpreted as the transit time of the radiation heat wave through the foil. After its onset the radiation intensity rises very sharply (within less than 200 ps) and reaches, for the example shown, the intensity radiated by the open hole (depending on the conditions, the intensity generally stays below that radiated by the open hole).

It may be interesting to note that the sharp onset of the radiation intensity was also observed in targets designed for generating Planck radiation under clean conditions¹⁵ (details will be published elsewhere). In these targets no laser light was radiated into the cavity carrying the gold foil. It was heated by laser-generated and reemitted x rays or only reemitted x rays through openings taking the place of the laser holes. This observation provides additional evidence that the observed phenomenon is indeed due to an x-ray-driven heat wave.

The experiment illustrated by Figs. 3(a) and 3(b) is now compared with the predictions of Eqs. (1) and (2). The average laser flux was $S_L = 2 \times 10^{14} \text{W cm}^{-2}$ and the pulse duration (FWHM) 0.8 ns. The intensity in the laser-irradiated zones on the inner wall of the cavity was

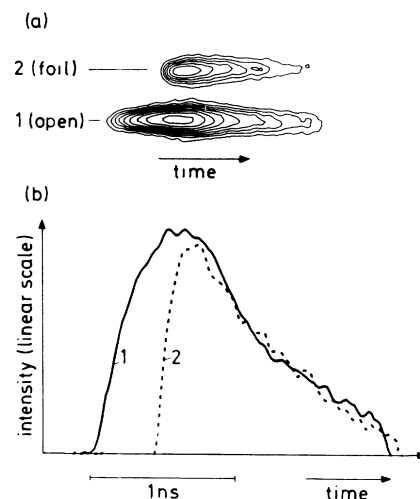


FIG. 3. (a) Isointensity contours on the screen of the XRSC. Observed wavelength 60 \AA ; 1-mm cavity with 0.91- μm gold foil. (b) X-ray intensity vs time from (a).

$1.3 \times 10^{15} \text{ W cm}^{-2}$. At this intensity conversion measurements¹⁶ in open geometry indicate a conversion efficiency into x rays of about 0.6. This yields an average source flux of $1.2 \times 10^{14} \text{ W cm}^{-2}$ in the cavity. For a 1-mm cavity with a fractional hole area $n^{-1} = 0.089$ one calculates a correction factor for the source flux of 0.73.

With these numbers one finds from Eqs. (1) and (2) a burnthrough time of 210 ps for a 0.91- μm -thick gold foil and a temperature of 245 eV at $t = 0.8 \text{ ns}$.

In the experiment the delay between the signal from the open hole and the foil is 430 ps at the base of the pulses and 330 ps at half maximum. A temperature of $230 \pm 15 \text{ eV}$ was measured at the time of maximum emission (the error margin is derived from an estimate of the accuracy of the film calibration). It is seen that in the experiment the propagation speed of the wave and the temperature are somewhat lower than predicted. This difference may be due in part to the fact that in Eqs. (1) and (2) the rise time of the pulse is not taken into account (they are derived for a temporally constant source flux), but it could also indicate that some of the underlying assumptions, e.g., about the x-ray conversion efficiency, material opacity, and complete thermodynamic equilibrium, do not completely conform to reality. Although we discuss here the comparison with the theory of a single representative shot, a similar agreement over the complete range of average laser flux and foil thicknesses used (data from the rest of the experiments) is observed. Indeed the agreement is better for the experiments performed with larger cavities at lower temperatures.

For a more quantitative analysis we have started to simulate the experiments in the multigroup diffusion approximation using the MULTI¹⁷ and ILESTA¹⁸ codes. Such simulations can take into account the real pulse shape, provide a more detailed description of radiative transport, and include the process of laser-light conversion. In the 1D (spherical) simulations a laser-irradiated gold sphere was located in the center of the cavity. Its surface area was equal to that of the laser-irradiated wall area in the experiment to warrant the correct laser intensity, which determines the conversion efficiency and the source spectrum. The wall thickness was either chosen equal to the foil thickness to simulate burnthrough, or thick (10 μm) to simulate the evolution of the radiation as seen through the open hole in the experimental cavity. The loss of radiation through holes was taken into account by an appropriate boundary condition in the innermost Lagrangian cell of the wall. A burnthrough simulation for the experiment of Fig. 3 is presented in Fig. 4. It shows the spatial and temporal evolutions of the flux of outward directed photons (wavelength interval 55–65 \AA) inside the heated foil. In this wavelength interval the radiation emitted through the outer surface of the foil rises very sharply after a delay of 500 ps. In a separate simulation the brightness tem-

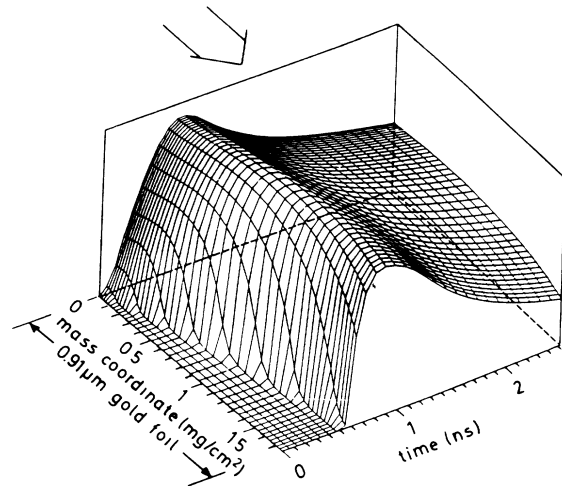


FIG. 4. Evolution of the flux of outward-directed photons in the wavelength interval 55–65 \AA inside the heated foil from a MULTI simulation of the experiment shown in Fig. 3. The vertical scale is linear.

perature of the radiation emitted from a thick outer wall into the cavity reached 220 eV at the time of maximum emission. Thus, the more realistic simulation is in very reasonable agreement with the experimentally measured burnthrough time and temperature. A full account of the experimental data and a more detailed comparison with simulation results will be published elsewhere.

In conclusion, the example of a radiation heat wave studied in this work makes it obvious that laser-heated cavities open new possibilities for the quantitative investigation of high-temperature hydrodynamic phenomena in the laboratory. Such studies are of interest for obtaining a basic insight into the state of matter at very high density and temperature and have potential applications to inertial-confinement fusion.

This work was supported in part by the Commission of the European Community in the framework of the Euratom-IPP Association and by Monbusho International Scientific Research Program.

(a) On leave from Department of Electrical Engineering, University of Alberta, Edmonton Alta., Canada T6G 2G7.

(b) On leave from Institute of Laser Engineering, Osaka University, Suita, Osaka 565, Japan.

¹R. E. Marshak, *Phys. Fluids* **1**, 24 (1958).

²Ya. B. Zel'dovich and Yu. P. Raizer, *Physics of Shock Waves and High-Temperature Hydrodynamic Phenomena* (Academic, New York, 1966).

³P. Herrmann, R. Pakula, I. B. Földes, R. Sigel, G. D. Tsakiris, and S. Witkowski, *Z. Naturforsch.* **41a**, 767 (1986).

⁴T. Mochizuki *et al.*, in *Proceedings of the Eleventh Inter-*

national Conference on Plasma Physics and Controlled Nuclear Fusion Research, Kyoto, Japan, 1986, edited by J. Weil and M. Demir (IAEA, Vienna, 1987), Vol. 3, p. 25.

⁵S. Sakabe, R. Sigel, G. D. Tsakiris, I. B. Földes, and P. Herrmann, *Phys. Rev. A* **38**, 5756 (1988).

⁶G. D. Tsakiris and R. Sigel, *Phys. Rev. A* **38**, 5769 (1988).

⁷G. D. Tsakiris, P. Herrmann, R. Pakula, R. Schmalz, R. Sigel, and S. Witkowski, *Europhys. Lett.* **2**, 213 (1986).

⁸R. Sigel, R. Pakula, S. Sakabe, and G. D. Tsakiris, *Phys. Rev. A* **38**, 5779 (1988).

⁹T. Mochizuki, K. Mima, N. Ikeda, R. Kodama, H. Shiraga, K. A. Tanaka, and C. Yamanaka, *Phys. Rev. A* **36**, 3279 (1987).

¹⁰P. Celliers and K. Eidmann, *Phys. Rev. A* **41**, 3270 (1990).

¹¹R. Pakula and R. Sigel, *Phys. Fluids* **28**, 232 (1985); **29**, 1340(E) (1986).

¹²R. Sigel, in *Laser Plasma Interactions 4*, edited by M. Hooper (SUSSP Publications, Edinburgh, 1989).

¹³G. D. Tsakiris and K. Eidmann, *J. Quant. Spectrosc. Radiat. Transfer* **38**, 353 (1987).

¹⁴K. Eidmann, T. Kishimoto, P. Herrmann, J. Mizui, R. Pakula, R. Sigel, and S. Witkowski, *Laser Part. Beams* **4**, 521 (1986).

¹⁵R. Sigel, J. Massen, and G. D. Tsakiris, in *Inertial Confinement Fusion*, Proceedings of the Course and Workshop of the International School of Plasma Physics "Piero Caldirola," Varenna, Italy, September 1988, edited by A. Caruso and E. Sindoni (Editrice Compositori, Bologna, 1989), p. 169.

¹⁶P. D. Goldstone, S. R. Goldman, W. C. Mead, J. A. Cobble, G. Stradling, R. H. Day, A. Hauer, M. C. Richardson, R. S. Marjoribanks, P. A. Jaanimagi, R. L. Keck, F. J. Marshall, W. Seka, O. Barnouin, B. Yaakobi, and S. A. Letzring, *Phys. Rev. Lett.* **59**, 56 (1987).

¹⁷R. Ramis, R. Schmalz, and J. Meyer-ter-Vehn, *Comput. Phys. Commun.* **49**, 475 (1988).

¹⁸H. Takabe *et al.*, *Phys. Fluids* **31**, 2884 (1988).